



## Manganese doping ordered mesoporous $\text{Co}_3\text{O}_4$ as heterogeneous peroxymonosulfate activator for the degradation of bisphenol A

Jing Deng<sup>a,b</sup>, Yongjian Ge<sup>b</sup>, Xiaoyan Ma<sup>b</sup>, Shanfang Feng<sup>b</sup>, Yijing Chen<sup>b</sup>, Yongqing Cheng<sup>b</sup>, Hongyu Wang<sup>b,\*</sup>

<sup>a</sup>College of Civil Engineering and Architecture, Zhejiang University, Hangzhou 310058, China

<sup>b</sup>College of Civil Engineering and Architecture, Zhejiang University of Technology, Hangzhou 310014, China, Tel./Fax: +86 571 88320180; email: hywangzjut@163.com (H. Wang)

Received 16 November 2016; Accepted 19 April 2017

### ABSTRACT

A novel catalyst,  $\text{Co}_3\text{O}_4\text{-CoMn}_2\text{O}_4$  in which manganese was doped into ordered mesoporous  $\text{Co}_3\text{O}_4$ , was synthesized and used as peroxymonosulfate (PMS) activation for the degradation of bisphenol A (BPA) in water. The effects of  $\text{Co}_3\text{O}_4\text{-CoMn}_2\text{O}_4$  dose, PMS concentration, solution pH, temperature and anions were also investigated. Results showed that higher catalyst loading, PMS concentration and reactive temperature would accelerate the BPA degradation, and  $\text{Co}_3\text{O}_4\text{-CoMn}_2\text{O}_4$  had a wide pH range in the activation of PMS.  $\text{Cl}^-$  and  $\text{H}_2\text{PO}_4^-$  could favor the BPA removal, whereas,  $\text{NO}_3^-$ ,  $\text{HCO}_3^-$  and  $\text{SO}_4^{2-}$  would inhibit it. Sulfate radicals were confirmed to be the major active species in the heterogeneous system through radicals quenching experiments. Catalytic activity in PMS solution was remained after five consecutive runs. Due to its lower toxicity and cost,  $\text{Co}_3\text{O}_4\text{-CoMn}_2\text{O}_4$  should be a promising catalyst applied in curbing environmental pollution.

**Keywords:**  $\text{Co}_3\text{O}_4\text{-CoMn}_2\text{O}_4$ ; Peroxymonosulfate; Bisphenol A; Degradation; Sulfate radicals

### 1. Introduction

Over the past years, various endocrine disrupting chemicals (EDCs) have been detected in surface water and became an environmental concern because it could cause a series of potential endangerment to humans and ecosystems [1–3]. Bisphenol A (BPA), 2,2'-bis(4-hydroxyphenyl) propane, one of the EDCs, has been widely used to produce polycarbonate plastics and epoxy resins, and it can be found everywhere in our daily life, such as electronic equipment, medical devices, toys, sports safety equipment, baby bottles, water pipes and so forth [4]. Certainly, it brought many benefits and conveniences to us, however, as a typical endocrine disruptor, it also resulted in a great deal of problems about environment pollution and human health which was frequently detected in surface water and groundwater around the world [4–6].

Even more serious is that traditional wastewater treatment process cannot remove it absolutely due to its high chemical stability [7]. Consequently, the method that can effectively eliminate BPA in water is urgently needed.

Sulfate radicals ( $\text{SO}_4^{\cdot-}$ ) have recently gained increasing attention among environmental researchers and showed the possibility for the replacement of hydroxyl radicals ( $\cdot\text{OH}$ ) in the field of advanced oxidation processes because of their comparative standard reduction potential, longer half-life, better selectivity for the target pollutants and wider operative pH ranges [8–10]. To date,  $\text{SO}_4^{\cdot-}$  can be generated from peroxymonosulfate (PMS) or persulfate (PS) decomposition activated by transition metals [8], ultraviolet [11–13], heat [14,15], ultrasound [16], base [17], anions [18] and some nonmetal materials [19–22]. It should be noticed that transition metals activated PMS or PS is more feasible than others for the lower energy demand and higher effectiveness. Especially,  $\text{Co}^{2+}$ /PMS system was an effective route for  $\text{SO}_4^{\cdot-}$  generation and contaminants degradation in water [23–24].

\* Corresponding author.

However,  $\text{Co}^{2+}$  is highly toxic to us and can cause secondary pollution in water. To overcome this problem, more researchers are inclined to use heterogeneous cobalt-based catalysts. Heterogeneous PMS activation through  $\text{Co}_3\text{O}_4$  was first attempted by Anipsitakis et al. [25], and gained desirable performance in the degradation of 2,4-dichlorophenol. Chen et al. [26] applied nano- $\text{Co}_3\text{O}_4$ /PMS system to investigate kinetics and mechanism using Acid Orange 7 as model compound, and presented prospect to us that use nano- $\text{Co}_3\text{O}_4$ /PMS system to degrade refractory organic contaminants.

Many researchers have put their focus on bimetallic oxides. Zhang et al. [27] incorporated Cu into mesoporous  $\text{MnO}_2$  to produce mesoporous Cu/ $\text{MnO}_2$  and demonstrated that it was a favorable catalyst in the Fenton-like reaction. Deng et al. [9] successfully synthesized  $\text{CoFe}_2\text{O}_4$  nanoparticles and proved it was an excellent PMS activator for the degradation of diclofenac. Ding et al. [28] first tried to use  $\text{CuFe}_2\text{O}_4$  nanoparticles to activate PMS and proposed it had promising potentials in the application of controlling pollution. Yao et al. [29] fabricated a series of nanosized  $\text{Co}_x\text{Mn}_{3-x}\text{O}_4$  and achieved high performance in the generation of  $\text{SO}_4^{\cdot-}$  in PMS solution. It could be seen that bimetallic oxides not only presented superior catalytic activity in PMS activation, but also suppressed the leaching of metallic ions because of intimate interactions between two metals, such as Fe–Co interactions in  $\text{CoFe}_2\text{O}_4$  [10]. In our preliminary research, ordered mesoporous  $\text{Co}_3\text{O}_4$  was synthesized and presented superior catalytic activity toward PMS than its spinel counterpart, however, the cobalt leaching of ordered mesoporous  $\text{Co}_3\text{O}_4$  was up to  $77.74 \mu\text{g}\cdot\text{L}^{-1}$ , higher than the conventional  $\text{Co}_3\text{O}_4$  nanoparticles [30]. It can be speculated that doping manganese to ordered mesoporous  $\text{Co}_3\text{O}_4$  can decrease the leakage of cobalt ions. In addition, it is well-known that manganese is ubiquitous in the earth, moderate in price and nontoxic to human.

Therefore, in order to decrease the danger of ordered mesoporous  $\text{Co}_3\text{O}_4$  in practical environmental cleanup, in this paper, we demonstrated a facile method to synthesize a novel catalyst,  $\text{Co}_3\text{O}_4\text{--CoMn}_2\text{O}_4$  in which manganese was incorporated into ordered mesoporous  $\text{Co}_3\text{O}_4$ . Through our study, this special material was applied in the PMS activation for the BPA degradation. Besides, the effects of several key parameters and interface mechanism were also discussed.

## 2. Experimental setup

### 2.1. Chemicals

The mesoporous silica KIT-6 was purchased from Nanjing XFNANO Materials Tech Co., Ltd. (Jiangsu, China). BPA and PMS (Oxone,  $\text{KHSO}_5\cdot 0.5\text{KHSO}_4\cdot 0.5\text{K}_2\text{SO}_4$ ,  $\text{KHSO}_5 \geq 47\%$ ) were obtained from Sigma-Aldrich Chemical Co., Ltd. (Shanghai, China). The other reagents were provided by Sinopharm Chemical Reagent Co., Ltd. (Shanghai, China). All the chemicals were used without further purification.

### 2.2. Synthesis process

#### 2.2.1. Preparation of ordered mesoporous $\text{Co}_3\text{O}_4$

KIT-6 and ethanol were served as hard template and solvent, respectively. Typically, 1.0 g KIT-6 was dispersed in ethanol solution of  $\text{Co}(\text{NO}_3)_2\cdot 6\text{H}_2\text{O}$  (0.8 M, 10 mL) and stirred for

1 h, then the mixture was dried at  $80^\circ\text{C}$  to evaporate ethanol and the resulting product was heated at  $200^\circ\text{C}$  for 6 h. The obtained powder was calcined at  $450^\circ\text{C}$  for 6 h (the heating rate was set at  $1^\circ\text{C}\cdot\text{min}^{-1}$ ), and then the template of resulting powder was removed by 2 M NaOH under water bath ( $80^\circ\text{C}$ ) with continuously stirring for 12 h. In order to ensure the complete removal of hard template, the process of removing template was repeated again. Finally, the black powder was washed with ethanol and distilled water several times until the pH of the filtrate reduced to near 7, and then dried overnight at  $60^\circ\text{C}$  under vacuum condition. The obtained ordered mesoporous  $\text{Co}_3\text{O}_4$  was denoted as OM- $\text{Co}_3\text{O}_4$ .

#### 2.2.2. Preparation of $\text{Co}_3\text{O}_4\text{--CoMn}_2\text{O}_4$

2.0 g as-prepared OM- $\text{Co}_3\text{O}_4$  was dispersed in ethanol of  $\text{Mn}(\text{NO}_3)_2\cdot 4\text{H}_2\text{O}$  (0.3 M, 10 mL) under magnetic stirring for 1 h, then the mixture was dried at  $60^\circ\text{C}$  and the black product was calcined at  $450^\circ\text{C}$  for 5 h (the heating rate was set at  $2^\circ\text{C}\cdot\text{min}^{-1}$ ). The black powder was triturated adequately for the subsequent experiments. The obtained powder was labeled as  $\text{Co}_3\text{O}_4\text{--CoMn}_2\text{O}_4$ .

#### 2.2.3. Characterization and analysis

X-ray diffraction (XRD) analysis was conducted on X'Pert PRO diffractometer (PANalytical, Holland) employing Cu  $\text{K}\alpha$  radiation. Transmission electron microscopy (TEM) images were performed on a Tecnai G<sup>2</sup> F30 S-Twin electron microscope (Philips, Holland). The specific surface area and pore-size distribution were determined from  $\text{N}_2$  physisorption data at 77 K obtained with ASAP 2010 analyzer (Micromeritics, USA). The pH at the point of zero charge ( $\text{pH}_{\text{pzc}}$ ) was measured by a zeta analyzer (Zetasizer Nano, Malvern, UK).

The change of BPA concentration was determined by high performance liquid chromatography (HPLC, Agilent 1200, USA) with an Eclipse XDB-C18 column ( $5 \mu\text{m}$ ,  $4.5 \times 150 \text{ mm}$ ) and a UV detector at  $\lambda = 270 \text{ nm}$ , the mobile phase was consisted of water and methanol (35/65 by v/v) with a flow rate of  $1 \text{ mL}\cdot\text{min}^{-1}$ . The pH value was determined by a pH meter (PHSJ-4F, Leici, China).

#### 2.2.4. Batch experiment

Batch experiments were carried out in a series of brown glass bottles that were installed in a constant temperature water bath apparatus (SHA-C, JiangNan Instrument Co., Ltd., Jiangsu, China). The temperature was set at  $25^\circ\text{C}$  except for considering the effect of reactive temperature. Typically for BPA degradation, an appropriate amount of catalysts were added into 100 mL BPA solution ( $20 \text{ mg}\cdot\text{L}^{-1}$ ) and stirred for 30 min to get adsorption–desorption equilibrium. PMS stock solution (100 mM) was prepared 30 min prior to reaction in case that PMS decayed before use. The reaction was started when appropriate volumes of the PMS stock solution were introduced.  $\text{H}_2\text{SO}_4$  and NaOH were employed to adjust the solution pH to a desirable level. At different time intervals, 1 mL samples were collected and filled with 100  $\mu\text{L}$   $\text{Na}_2\text{S}_2\text{O}_3$  solution (100 mM) to quench the reaction. Then, the samples were filtered by  $0.22 \mu\text{m}$  membrane for further analysis. After each experiment,  $\text{Co}_3\text{O}_4\text{--CoMn}_2\text{O}_4$  was collected from solution

by filtration, then washed with distilled water and ethanol several times, and dried in 70°C for the next runs to study the reusability of catalyst. Different anions including  $\text{SO}_4^{2-}$ ,  $\text{NO}_3^-$ ,  $\text{Cl}^-$ ,  $\text{HCO}_3^-$  and  $\text{H}_2\text{PO}_4^-$  were added into the  $\text{Co}_3\text{O}_4$ - $\text{CoMn}_2\text{O}_4$ /PMS system to investigate their effects in BPA degradation. All the experiments were carried out in duplicates, the reported data in this paper were means of the two independent measurements. And the standard deviations were also calculated from the two independent measurements.

### 3. Results and discussion

#### 3.1. Characterization of catalysts

Fig. 1 shows XRD patterns of as-prepared catalysts. In the diffractogram of  $\text{OM-Co}_3\text{O}_4$ , the diffraction peaks appear at  $2\theta = 19.0^\circ, 31.4^\circ, 36.9^\circ, 37.9^\circ, 44.9^\circ, 55.7^\circ, 59.4^\circ$  and  $65.3^\circ$ , which attribute to (111), (220), (311), (222), (400), (422), (511) and (440), respectively, implying the formation of spinel  $\text{Co}_3\text{O}_4$  (JCPDS NO. 42-1467). However, as for  $\text{Co}_3\text{O}_4$ - $\text{CoMn}_2\text{O}_4$ , no significant difference was observed with  $\text{OM-Co}_3\text{O}_4$ , which might result from the lattice parameters of  $\text{CoMn}_2\text{O}_4$  are closely analogous with  $\text{Co}_3\text{O}_4$  [31]. The mean crystallite sizes can be calculated based on Debye–Scherrer equation, and the value of  $\text{Co}_3\text{O}_4$ - $\text{CoMn}_2\text{O}_4$  is calculated to be 19.76 nm, which is higher than that of  $\text{OM-Co}_3\text{O}_4$  (17.43 nm), suggesting that  $\text{CoMn}_2\text{O}_4$  is emerged in the boundaries and interstices of  $\text{OM-Co}_3\text{O}_4$ . And the crystallite size was listed in Table 1.

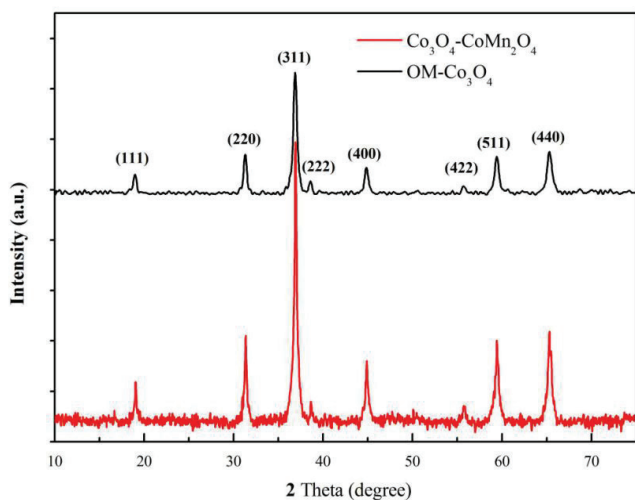


Fig. 1. XRD patterns of  $\text{OM-Co}_3\text{O}_4$  and  $\text{Co}_3\text{O}_4$ - $\text{CoMn}_2\text{O}_4$ .

Table 1  
Textural properties of  $\text{OM-Co}_3\text{O}_4$  and  $\text{Co}_3\text{O}_4$ - $\text{CoMn}_2\text{O}_4$

Samples	XRD Crystallite size (nm)	Nitrogen adsorption/desorption		
		BET ( $\text{m}^2\cdot\text{g}^{-1}$ )	Pore volume ( $\text{cm}^3\cdot\text{g}^{-1}$ )	Pore diameter (nm)
$\text{OM-Co}_3\text{O}_4$	17.43	66.9	0.135	8.08
$\text{Co}_3\text{O}_4$ - $\text{CoMn}_2\text{O}_4$	19.76	64.0	0.134	7.66

The morphologies and structures of  $\text{OM-Co}_3\text{O}_4$  and  $\text{Co}_3\text{O}_4$ - $\text{CoMn}_2\text{O}_4$  were presented by TEM and HR-TEM. As shown in Fig. 2(a),  $\text{OM-Co}_3\text{O}_4$  appears the feature of highly ordered mesoporous, which corresponds to mesoporous channels of KIT-6 template, and the pore size is close to 10 nm. When the manganese was doped into  $\text{OM-Co}_3\text{O}_4$  to synthesize  $\text{Co}_3\text{O}_4$ - $\text{CoMn}_2\text{O}_4$ , the ordered mesoporous structure has been destroyed in some regions (Fig. 2(c)) for the formation of  $\text{CoMn}_2\text{O}_4$  [31]. According to Fig. 2(b), the lattice fringes emerge clearly in HR-TEM image, and the adjacent lattice fringe spacings are 0.467 and 0.285 nm, corresponding to (111) and (220) crystal planes, respectively. Nevertheless, the lattice fringes are not apparent in Fig. 2(d), only the (220) plane can be observed.

In order to determine the Brunauer–Emmett–Teller (BET) surface area and pore-size distribution, the  $\text{N}_2$  adsorption/desorption isotherms were carried out, and the curves can be seen in Fig. 3. Obviously, the isotherms of  $\text{OM-Co}_3\text{O}_4$  and  $\text{Co}_3\text{O}_4$ - $\text{CoMn}_2\text{O}_4$  demonstrate type IV isotherms with hysteresis loops, indicating obtention of mesoporous structure, are in accord with TEM images. The pore-size distribution of  $\text{Co}_3\text{O}_4$ - $\text{CoMn}_2\text{O}_4$  bears a resemblance to  $\text{OM-Co}_3\text{O}_4$ . The mean pore diameter of  $\text{OM-Co}_3\text{O}_4$  is 8.08 nm, which is a bit higher than that of  $\text{Co}_3\text{O}_4$ - $\text{CoMn}_2\text{O}_4$  (7.66 nm). The specific surface area and pore volume of  $\text{Co}_3\text{O}_4$ - $\text{CoMn}_2\text{O}_4$  are  $64.0 \text{ m}^2\cdot\text{g}^{-1}$  and  $0.134 \text{ cm}^3\cdot\text{g}^{-1}$ , respectively, which is slightly less than  $\text{OM-Co}_3\text{O}_4$ . The introduction of manganese leads to the shrink of channels in the  $\text{OM-Co}_3\text{O}_4$ , which causes the reduction of the specific surface area and mean pore diameter in  $\text{Co}_3\text{O}_4$ - $\text{CoMn}_2\text{O}_4$ . The BET surface area, pore volume and pore diameter were summarized in Table 1.

#### 3.2. Catalytic degradation of BPA

The BPA removal in various reaction conditions was first investigated. As depicted in Fig. 4, only 3% BPA could be oxidized with PMS alone for 1 h, suggesting that active radicals cannot be generated by PMS alone at room temperature. With only  $\text{Co}_3\text{O}_4$ - $\text{CoMn}_2\text{O}_4$ , there was no significant change in BPA concentration, indicating that the adsorption on the  $\text{Co}_3\text{O}_4$ - $\text{CoMn}_2\text{O}_4$  surface could be negligible. However, almost all of BPA was removed for 60 min in the  $\text{Co}_3\text{O}_4$ - $\text{CoMn}_2\text{O}_4$ /PMS system. The result shows that  $\text{Co}_3\text{O}_4$ - $\text{CoMn}_2\text{O}_4$  could stimulate PMS to produce reactive species, such as  $\cdot\text{OH}$  and  $\text{SO}_4^{\cdot-}$ . Moreover,  $\text{Co}_3\text{O}_4$ - $\text{CoMn}_2\text{O}_4$  presented the lower activity toward PMS activation than  $\text{OM-Co}_3\text{O}_4$ , it may result from the decreasing of BET surface area which caused by the introduction of manganese. But the intimate interactions between Co and Mn could suppress the cobalt leaching [10]. Therefore,  $\text{Co}_3\text{O}_4$ - $\text{CoMn}_2\text{O}_4$  may possess a greater potential in practical environmental cleanup than  $\text{OM-Co}_3\text{O}_4$ .

The reaction kinetics of BPA decay in the  $\text{Co}_3\text{O}_4$ - $\text{CoMn}_2\text{O}_4$ /PMS system could be fitted by pseudo-first-order kinetics (inset of Fig. 4):

$$\ln\left(\frac{[\text{BPA}]}{[\text{BPA}]_0}\right) = -k_{\text{app}}t \quad (1)$$

where  $[\text{BPA}]_0$  ( $\text{mg}\cdot\text{L}^{-1}$ ) is the initial concentration of BPA,  $[\text{BPA}]$  ( $\text{mg}\cdot\text{L}^{-1}$ ) is the concentration at any specific time ( $t$ ) and  $k_{\text{app}}$  is the reaction rate constant ( $\text{min}^{-1}$ ). After calculation,

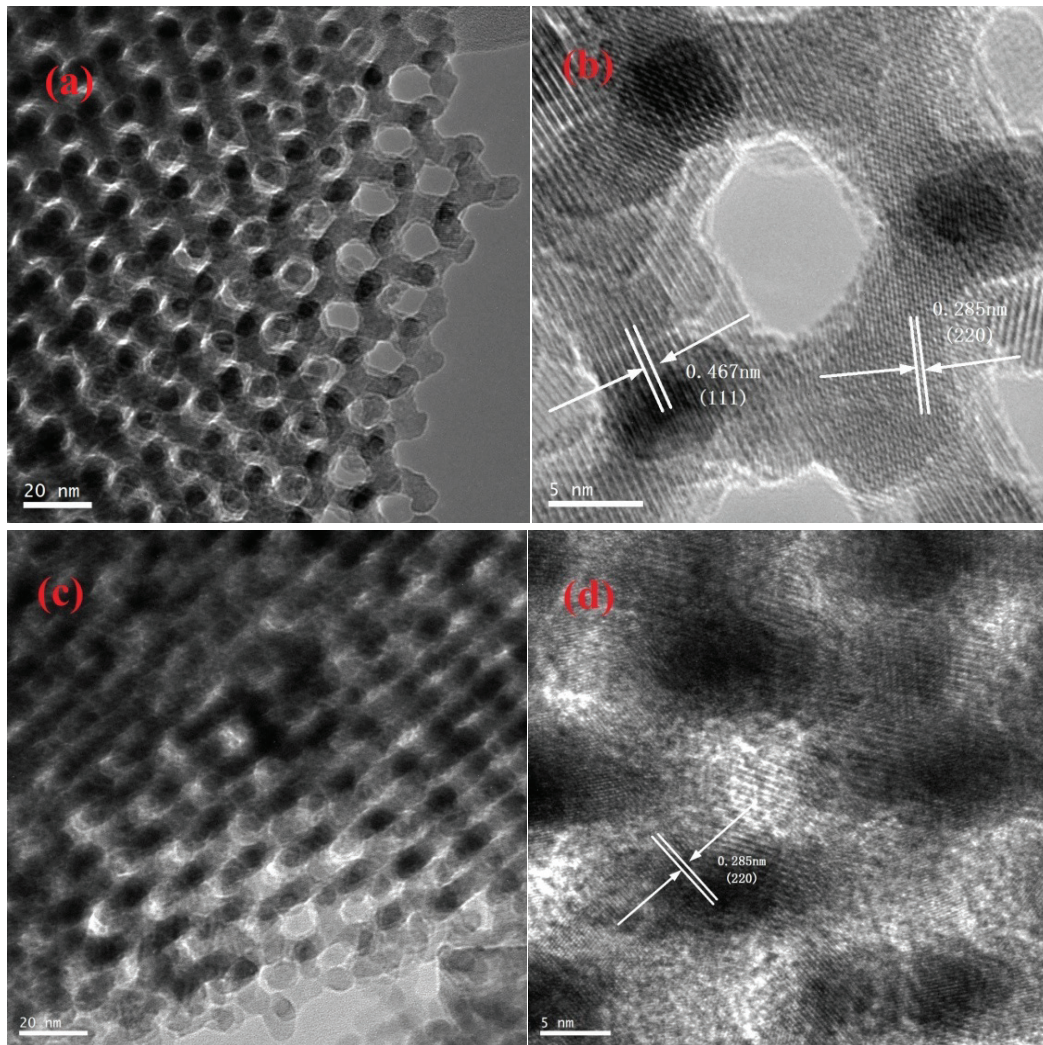


Fig. 2. TEM and HR-TEM images of (a) and (b) OM-Co<sub>3</sub>O<sub>4</sub>; and (c) and (d) Co<sub>3</sub>O<sub>4</sub>-CoMn<sub>2</sub>O<sub>4</sub>.

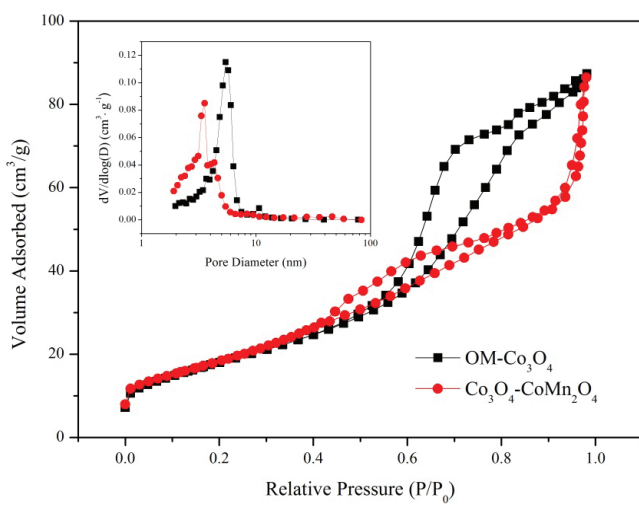


Fig. 3. N<sub>2</sub> adsorption-desorption isotherms and pore-size distributions (inset) of OM-Co<sub>3</sub>O<sub>4</sub> and Co<sub>3</sub>O<sub>4</sub>-CoMn<sub>2</sub>O<sub>4</sub>.

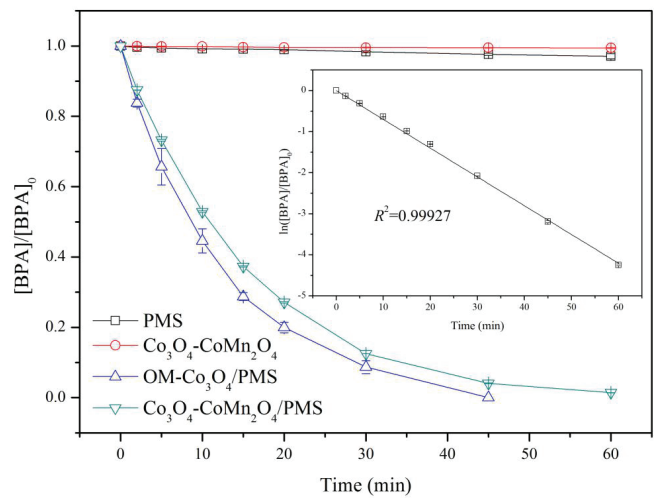


Fig. 4. BPA removal in different reaction conditions. Experimental condition: [BPA]<sub>0</sub> = 20 mg·L<sup>-1</sup>, [PMS]<sub>0</sub> = 0.5 mM, [Co<sub>3</sub>O<sub>4</sub>-CoMn<sub>2</sub>O<sub>4</sub>]<sub>0</sub> = 0.05 g·L<sup>-1</sup>, T = 25 °C.

the value of  $k_{app}$  is  $0.0701 \text{ min}^{-1}$  in the  $\text{Co}_3\text{O}_4\text{-CoMn}_2\text{O}_4/\text{PMS}$  system. The BPA degradation kinetic data under different experimental conditions was summarized in Table 2.

### 3.3. Identification of primary reactive species and possible catalytic mechanism

Three radicals may generate in heterogeneous PMS system, namely  $\cdot\text{OH}$ ,  $\text{SO}_4^{\cdot-}$  and  $\text{SO}_5^{\cdot-}$  [32]. Due to its low oxidative capacity ( $E(\text{SO}_5^{\cdot-}/\text{SO}_4^{2-}) = 1.1 \text{ V}$ ),  $\text{SO}_5^{\cdot-}$  can be excluded from primary species [28]. It is well known that *tert*-butyl alcohol (TBA) is an effective quenching agent for  $\cdot\text{OH}$  but not for  $\text{SO}_4^{\cdot-}$  ( $k_{\text{OH}} = 3.8\text{--}7.6 \times 10^8 \text{ M}^{-1} \text{ s}^{-1}$ ,  $k_{\text{SO}_4^{\cdot-}} = 4\text{--}9.1 \times 10^5 \text{ M}^{-1} \text{ s}^{-1}$ ) [33], while

ethanol (EtOH) is a well scavenger for  $\text{SO}_4^{\cdot-}$  and  $\cdot\text{OH}$  ( $k_{\text{SO}_4^{\cdot-}} = 1.6\text{--}7.7 \times 10^7 \text{ M}^{-1} \text{ s}^{-1}$ ,  $k_{\text{OH}} = 1.2\text{--}2.8 \times 10^9 \text{ M}^{-1} \text{ s}^{-1}$ ) [8]. Consequently, EtOH and TBA were employed as the radical quenching agents to identify the primary active radicals.

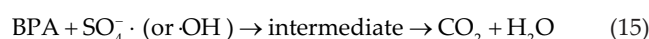
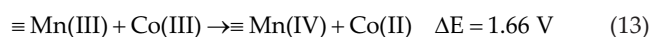
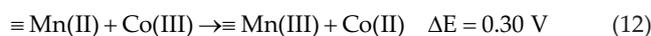
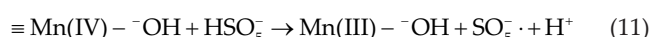
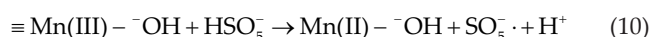
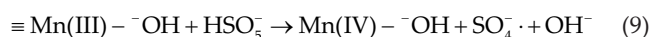
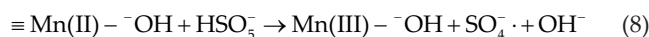
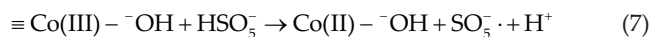
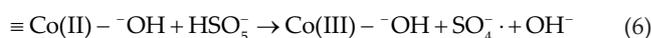
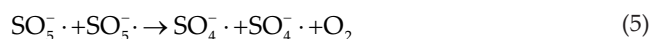
As exhibited in Fig. 5, the removal rate of BPA was 98.4% in 60 min with no scavenger in the system, and when 10 and 100 mM TBA were added to the system, there was no obvious change in BPA removal. However, the BPA degradation would be strongly inhibited in the presence of EtOH. When 10 mM EtOH was added to the  $\text{Co}_3\text{O}_4\text{-CoMn}_2\text{O}_4/\text{PMS}$  system, the BPA removal was decreased to 88.1%, and the inhibition would be more significant with the increasing of EtOH concentration to 100 mM. Therefore, it can safely concluded

Table 2  
The BPA degradation kinetic data under different experimental conditions

S. No.	Experimental conditions	$k_{app}$ ( $\text{min}^{-1}$ )	$t_{1/2}$ (min)	$R^2$
[BPA] <sub>0</sub> = 20 mg·L <sup>-1</sup> , [PMS] = 0.5 mM, [Co <sub>3</sub> O <sub>4</sub> -CoMn <sub>2</sub> O <sub>4</sub> ] = 0.05 g·L <sup>-1</sup> , T = 25°C				
1	None	0.070	9.902	0.999
2	EtOH = 10 mM	0.038	18.241	0.994
3	EtOH = 100 mM	0.017	40.773	0.946
4	TBA = 10 mM	0.069	10.046	0.996
5	TBA = 100 mM	0.068	10.193	0.997
[BPA] <sub>0</sub> = 20 mg·L <sup>-1</sup> , [PMS] = 0.5 mM, [Co <sub>3</sub> O <sub>4</sub> -CoMn <sub>2</sub> O <sub>4</sub> ] = 0.01–0.15 g·L <sup>-1</sup> , T = 25°C				
1	[Co <sub>3</sub> O <sub>4</sub> -CoMn <sub>2</sub> O <sub>4</sub> ] = 0.01 g·L <sup>-1</sup>	0.014	49.511	0.999
2	[Co <sub>3</sub> O <sub>4</sub> -CoMn <sub>2</sub> O <sub>4</sub> ] = 0.025 g·L <sup>-1</sup>	0.028	24.755	0.999
3	[Co <sub>3</sub> O <sub>4</sub> -CoMn <sub>2</sub> O <sub>4</sub> ] = 0.05 g·L <sup>-1</sup>	0.070	9.902	0.999
4	[Co <sub>3</sub> O <sub>4</sub> -CoMn <sub>2</sub> O <sub>4</sub> ] = 0.075 g·L <sup>-1</sup>	0.106	6.539	0.995
5	[Co <sub>3</sub> O <sub>4</sub> -CoMn <sub>2</sub> O <sub>4</sub> ] = 0.15 g·L <sup>-1</sup>	0.262	2.646	0.995
[BPA] <sub>0</sub> = 20 mg·L <sup>-1</sup> , [PMS] = 0.1–1.5 mM, [Co <sub>3</sub> O <sub>4</sub> -CoMn <sub>2</sub> O <sub>4</sub> ] = 0.05 g·L <sup>-1</sup> , T = 25°C				
1	[PMS] = 0.1 mM	0.033	21.004	0.992
2	[PMS] = 0.25 mM	0.055	12.603	0.999
3	[PMS] = 0.5 mM	0.070	9.902	0.999
4	[PMS] = 0.75 mM	0.072	9.627	0.998
5	[PMS] = 1.5 mM	0.080	8.664	0.997
[BPA] <sub>0</sub> = 20 mg·L <sup>-1</sup> , [PMS] = 0.5 mM, [Co <sub>3</sub> O <sub>4</sub> -CoMn <sub>2</sub> O <sub>4</sub> ] = 0.05 g·L <sup>-1</sup> , pH = 3–11, T = 25°C				
1	pH = 3	0.033	21.004	0.997
2	pH = 5	0.074	9.367	0.996
3	pH = 7	0.074	9.367	0.997
4	pH = 9	0.073	9.495	0.997
5	pH = 11	0.02	34.657	0.969
[BPA] <sub>0</sub> = 20 mg·L <sup>-1</sup> , [PMS] = 0.5 mM, [Co <sub>3</sub> O <sub>4</sub> -CoMn <sub>2</sub> O <sub>4</sub> ] = 0.05 g·L <sup>-1</sup> , T = 25°C–65°C				
1	T = 25°C	0.070	9.902	0.998
2	T = 35°C	0.171	4.054	0.994
3	T = 45°C	0.292	2.374	0.998
4	T = 55°C	0.483	1.435	0.997
5	T = 65°C	0.700	0.990	0.999
[BPA] <sub>0</sub> = 20 mg·L <sup>-1</sup> , [PMS] = 0.5 mM, [Co <sub>3</sub> O <sub>4</sub> -CoMn <sub>2</sub> O <sub>4</sub> ] = 0.05 mg·L <sup>-1</sup> , T = 25°C				
1	None	0.070	9.902	0.999
3	[SO <sub>4</sub> <sup>2-</sup> ] = 10 mM	0.039	17.773	0.992
4	[NO <sub>3</sub> <sup>-</sup> ] = 10 mM	0.032	21.661	0.997
5	[Cl <sup>-</sup> ] = 10 mM	0.131	5.291	0.994
6	[HCO <sub>3</sub> <sup>-</sup> ] = 10 mM	0.010	69.315	0.834
7	[H <sub>2</sub> PO <sub>4</sub> <sup>-</sup> ] = 10 mM	0.358	1.936	0.996

that  $\text{SO}_4^{\cdot-}$  is the dominated species and a small amount of  $\cdot\text{OH}$  coexists in the  $\text{Co}_3\text{O}_4\text{-CoMn}_2\text{O}_4/\text{PMS}$  system. Similar findings were reported in  $\text{CuFe}_2\text{O}_4$  nanoparticles activated PMS to remove iopromide and tetrabromobisphenol A in water [28,34].

On the basis of the experimental result, a possible mechanism of heterogeneous PMS activation by  $\text{Co}_3\text{O}_4\text{-CoMn}_2\text{O}_4$  was proposed. First,  $\equiv\text{Co(II)}$  and  $\equiv\text{Mn(II)}$  combined with dissociative  $\text{H}_2\text{O}$  molecules adsorbed on the catalyst surface to generate  $\equiv\text{Co(II)-OH}$  and  $\equiv\text{Mn(II)-OH}$  [35,36]. After introduction of PMS,  $\equiv\text{Co(II)}$  and  $\equiv\text{Mn(II)}$  will react with  $\text{HSO}_5^-$  to produce  $\cdot\text{OH}$  (Eqs. (2) and (3)), and then  $\text{SO}_4^{\cdot-}$  would be generated through some  $\cdot\text{OH}$  species reacted with  $\text{HSO}_5^-$  (Eqs. (4) and (5)) [37]. On the other hand, the generation of  $\text{SO}_4^{\cdot-}$  could occur on the  $\text{Co}_3\text{O}_4\text{-CoMn}_2\text{O}_4$  surface by  $\equiv\text{Co(II)-OH}$  reacted with PMS (Eq. (6)), and the reaction product ( $\equiv\text{Co(III)-OH}$ ) would also react with PMS to produce  $\equiv\text{Co(II)-OH}$  (Eq. (7)) [29]. Similarly, PMS can also be activated by  $\equiv\text{Mn(II)-OH}$  and  $\equiv\text{Mn(III)-OH}$  on the  $\text{Co}_3\text{O}_4\text{-CoMn}_2\text{O}_4$  surface and decomposed to produce  $\text{SO}_4^{\cdot-}$  (Eqs. (8) and (9)), and more  $\equiv\text{Mn(II)-OH}$  and  $\equiv\text{Mn(III)-OH}$  will be produced through formed  $\equiv\text{Mn(III)-OH}$  and  $\equiv\text{Mn(IV)-OH}$  reacted with  $\text{HSO}_5^-$  (Eqs. (10) and (11)). Furthermore, due to higher standard reduction potential of  $\text{Co}^{3+}/\text{Co}^{2+}$  (1.81 V) than  $\text{Mn}^{3+}/\text{Mn}^{2+}$  (1.15 V) and  $\text{MnO}_2/\text{Mn}_2\text{O}_3$  (0.15 V) [29,38], the reduction of  $\text{Co}^{3+}$  by  $\text{Mn}^{2+}$  and  $\text{Mn}^{3+}$  is thermodynamically favorable (Eqs. (12) and (13)) [29]. It means that a regular catalytic cycle would persist on the surface of  $\text{Co}_3\text{O}_4\text{-CoMn}_2\text{O}_4$ . In addition, the reaction between  $\text{SO}_4^{\cdot-}$  and  $\text{OH}^-$  could also exist in the system, and  $\cdot\text{OH}$  would be generated in the system (Eq. (14)) [39].  $\text{SO}_4^{\cdot-}$  and  $\cdot\text{OH}$  continuously attacked BPA until BPA was decomposed completely (Eq. (15)).



### 3.4. Effect of $\text{Co}_3\text{O}_4\text{-CoMn}_2\text{O}_4$ dosage

A series of experiments were conducted with different doses of  $\text{Co}_3\text{O}_4\text{-CoMn}_2\text{O}_4$  ranging from 0.01 to 0.15  $\text{g}\cdot\text{L}^{-1}$  to investigate the effect of  $\text{Co}_3\text{O}_4\text{-CoMn}_2\text{O}_4$  dosage on BPA removal, and the result is shown in Fig. 6. In accordance with expectation, the increasing of catalyst dosage would promote the BPA degradation. When the dose of  $\text{Co}_3\text{O}_4\text{-CoMn}_2\text{O}_4$  increased from 0.01 to 0.15  $\text{g}\cdot\text{L}^{-1}$ , the value of  $k_{\text{app}}$  increased from 0.014 to 0.262  $\text{min}^{-1}$ . The increase of  $\text{Co}_3\text{O}_4\text{-CoMn}_2\text{O}_4$  dosage would enhance the odds of contact between  $\text{Co}_3\text{O}_4\text{-CoMn}_2\text{O}_4$  and PMS, and more radicals

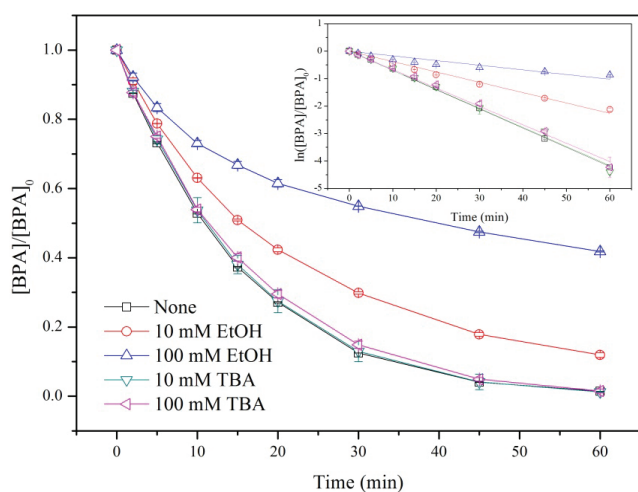


Fig. 5. The effect of different quenchers (TBA and EtOH) on BPA removal. Experimental condition:  $[\text{BPA}]_0 = 20 \text{ mg}\cdot\text{L}^{-1}$ ,  $[\text{PMS}]_0 = 0.5 \text{ mM}$ ,  $[\text{Co}_3\text{O}_4\text{-CoMn}_2\text{O}_4]_0 = 0.05 \text{ g}\cdot\text{L}^{-1}$ ,  $T = 25^\circ\text{C}$ .

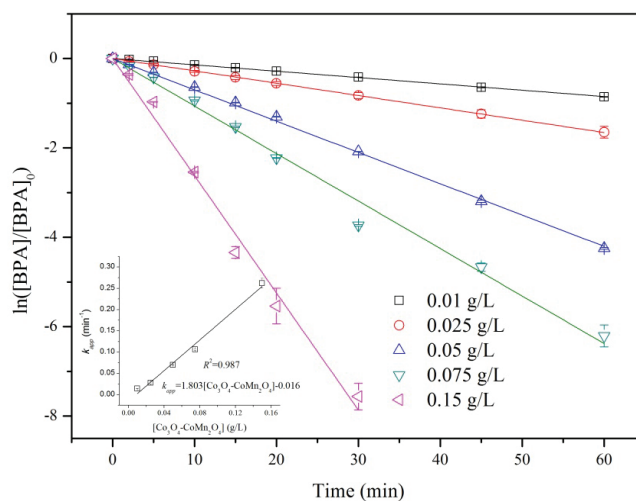
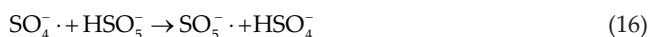


Fig. 6. The effect of  $\text{Co}_3\text{O}_4\text{-CoMn}_2\text{O}_4$  dosage on BPA removal. Experimental condition:  $[\text{BPA}]_0 = 20 \text{ mg}\cdot\text{L}^{-1}$ ,  $[\text{PMS}]_0 = 0.5 \text{ mM}$ ,  $[\text{Co}_3\text{O}_4\text{-CoMn}_2\text{O}_4]_0 = 0.01\text{-}0.15 \text{ g}\cdot\text{L}^{-1}$ ,  $T = 25^\circ\text{C}$ .

would be generated and accelerated the BPA removal. The phenomenon can be found generally in other heterogeneous PMS systems, such as  $\text{Mn}_2\text{O}_3/\text{PMS}$  and  $\text{CoFe}_2\text{O}_4/\text{TNTs}/\text{PMS}$  processes [40,41]. The linear relationship between the values of  $k_{\text{app}}$  and the  $\text{Co}_3\text{O}_4\text{-CoMn}_2\text{O}_4$  loading could be established:  $k_{\text{app}} = 1.803 \times [\text{Co}_3\text{O}_4\text{-CoMn}_2\text{O}_4] - 0.016$ , the curve is plotted in the inset of Fig. 6. The linear relationship between  $k_{\text{app}}$  and catalyst dosage in heterogeneous PMS system to remove organic pollutants were also reported in previous investigations [28,42].

### 3.5. Effect of PMS concentration

A series of experiments were conducted with different initial PMS concentrations ranging from 0.1 to 1.5 mM to investigate the effect of PMS concentration on BPA removal, and the result was exhibited in Fig. 7. It was not difficult to find that the BPA degradation increased with the enhancement of PMS concentration. However, unlike the effect of catalyst dosage above, there was no linear relationship between  $k_{\text{app}}$  and the PMS concentration. When the PMS concentration exceeded 0.5 mM, the growth of  $k_{\text{app}}$  slowed down. Similar consequent was reported in Orange II oxidation in the  $\text{MnFe}_2\text{O}_4/\text{PMS}$  system [33] and dimethyl phthalate degradation by graphene-based  $\text{CoFe}_2\text{O}_4$  activated PMS [43]. Obviously, as the origin of active radicals, the increase of initial PMS concentration generates more  $\text{SO}_4^{\cdot-}$  and  $\cdot\text{OH}$ , consequently improves the BPA degradation. However, the extra PMS can behave as a scavenger to quench radicals (Eqs. (4) and (16)) when further increase the PMS concentration [44].



### 3.6. Effect of pH

A series of experiments were conducted with different initial pH values ranging from 3 to 11 for studying the effect of pH on BPA removal, and the result is illustrated in Fig. 8(a). Explicitly, the BPA degradation was largely influenced by solution pH, and the best BPA removal occurred in the pH ranging from 5 to 9. However, the BPA degradation would be greatly inhibited under alkaline conditions, which might be attributed to the following two factors. The  $\text{pH}_{\text{pzc}}$  of  $\text{Co}_3\text{O}_4\text{-CoMn}_2\text{O}_4$  after measured was 3.71, which means the  $\text{Co}_3\text{O}_4\text{-CoMn}_2\text{O}_4$  surface is negatively charged when solution pH is greater than 3.71. Hence, the electrostatic force repels negative anion, such as  $\text{HSO}_5^-$ , thereby, hinders the generation of  $\text{SO}_4^{\cdot-}$ . Under stronger alkaline condition, the electronic force becomes stronger in that the  $\text{SO}_5^{2-}$  is the dominant anion when  $\text{pH} > 9.4$  [45]. In addition,  $\text{SO}_4^{\cdot-}$  can react with  $\text{OH}^-$  and produce  $\cdot\text{OH}$  which possesses lower oxidation capacity (Eqs. (14) and (17)) [39]. At acid solution, the effect of H-bond would become more significant, suggesting the interaction between  $\text{HSO}_5^-$  and positively charge catalyst surface would be more difficult [34]. Therefore, the BPA removal would also be inhibited.

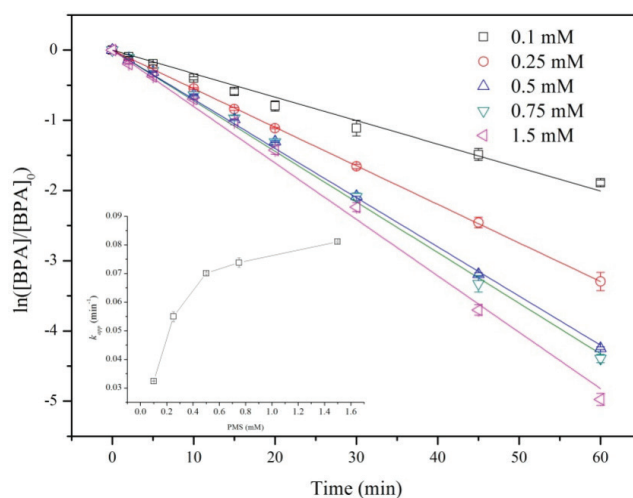


Fig. 7. The effect of initial PMS concentration on BPA removal. Experimental condition:  $[\text{BPA}]_0 = 20 \text{ mg}\cdot\text{L}^{-1}$ ,  $[\text{PMS}]_0 = 0.1\text{--}1.5 \text{ mM}$ ,  $[\text{Co}_3\text{O}_4\text{-CoMn}_2\text{O}_4]_0 = 0.05 \text{ g}\cdot\text{L}^{-1}$ ,  $T = 25^\circ\text{C}$ .

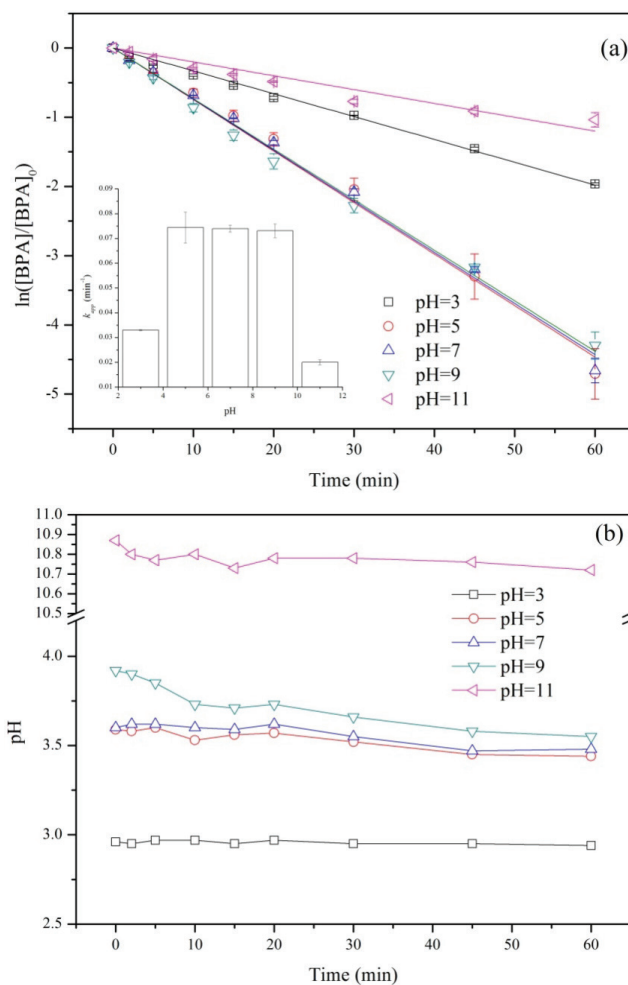


Fig. 8. (a) The effect of pH on BPA removal. (b) The variations of pH in the  $\text{Co}_3\text{O}_4\text{-CoMn}_2\text{O}_4/\text{PMS}$  system. Experimental condition:  $[\text{BPA}]_0 = 20 \text{ mg}\cdot\text{L}^{-1}$ ,  $[\text{PMS}] = 0.5 \text{ mM}$ ,  $[\text{Co}_3\text{O}_4\text{-CoMn}_2\text{O}_4] = 0.05 \text{ g}\cdot\text{L}^{-1}$ ,  $[\text{pH}] = 3\text{--}11$ ,  $T = 25^\circ\text{C}$ .

In addition, the variations of pH with reaction time in the  $\text{Co}_3\text{O}_4\text{-CoMn}_2\text{O}_4/\text{PMS}$  system were also investigated. It was reported that  $\text{HSO}_5^-$  is a weak acid with  $\text{p}K_a = 9.4$  [45], so the pH would change at once after addition of PMS in the solution, which also means that the pH at 0 min is not the value adjusted before. According to Fig. 8(b), the different initial pH presented different tendencies. When the initial pH was set at 3, the acidity in the process would keep around the original value. When the initial pH was changed to 11, the value of pH will decline a little and then stop around 10.7 in the process of BPA degradation. When the initial pH was 5, 7 or 9, the value of pH would decrease rapidly and then all steady around 3.5 in the process of BPA degradation. It might be contribute to the generation of organic acid during the course of BPA degradation and accumulation of  $\text{H}^+$  in the process of PMS activation [46]. Under the strong alkaline conditions, the difficulty of PMS activation will lead to less organic acid generation and  $\text{H}^+$  accumulation, which resulted in the slight change of solution pH.

### 3.7. Effect of temperature

A series of experiments were conducted with different temperatures ranging from 25°C to 65°C for investigating the effect of reactive temperature on BPA degradation, and the result is depicted in Fig. 9. The BPA degradation could be described by pseudo-first-order kinetics in different temperature conditions, it could be seen that the temperature positively influenced the degradation of BPA, the values of  $k_{\text{app}}$  increased from 0.070 to 0.700  $\text{min}^{-1}$  with increasing temperature from

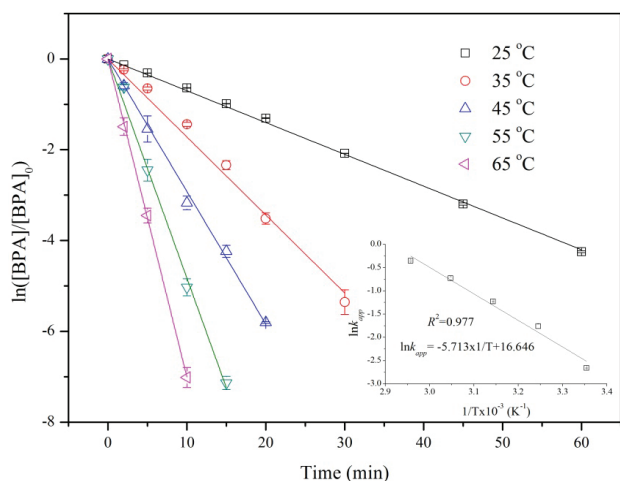


Fig. 9. The effect of temperature on BPA removal. Experimental condition:  $[\text{BPA}]_0 = 20 \text{ mg}\cdot\text{L}^{-1}$ ,  $[\text{PMS}]_0 = 0.5 \text{ mM}$ ,  $[\text{Co}_3\text{O}_4\text{-CoMn}_2\text{O}_4]_0 = 0.05 \text{ g}\cdot\text{L}^{-1}$ ,  $T = 25^\circ\text{C}\text{-}65^\circ\text{C}$ .

25°C to 65°C. The molecular collision will enhance in a high temperature [47], and a high temperature is benefited for reactant molecular to conquer activation energy barrier [48]. Furthermore, the inset of Fig. 9 presents a good linear correlation between  $\ln k_{\text{app}}$  and  $1/T$ , indicating that Arrhenius equation could be used in the  $\text{Co}_3\text{O}_4\text{-CoMn}_2\text{O}_4/\text{PMS}$  process:

$$\ln k_{\text{app}} = \ln A - E_a/RT \quad (18)$$

where  $k_{\text{app}}$  is the reaction rate constant ( $\text{min}^{-1}$ ),  $A$  is Arrhenius constant ( $\text{kJ}\cdot\text{mol}^{-1}$ ),  $E_a$  is activation energy ( $\text{kJ}\cdot\text{mol}^{-1}$ ),  $R$  is the universal gas constant ( $8.314\text{J}\cdot(\text{mol}\cdot\text{K})^{-1}$ ) and  $T$  is thermodynamic temperature (K). The activation energy was determined to be  $47.498 \text{ kJ}\cdot\text{mol}^{-1}$ , which was lower than BPA degradation in the  $\text{CoMnAl}$ -mixed metal oxides/PMS process ( $96.83 \text{ kJ}\cdot\text{mol}^{-1}$ ) [49] and phenol decomposition in the  $\text{Co}/\text{activated carbon-PMS}$  system ( $57.7 \text{ kJ}\cdot\text{mol}^{-1}$ ) [50], which means that the heterogeneous activation by  $\text{Co}_3\text{O}_4\text{-CoMn}_2\text{O}_4$  can occur at a lower energy.

### 3.8. Effect of anions

Inorganic anions are ubiquitous in the natural water. Thus, a series of experiments were conducted to study the effect of common coexist anions on BPA degradation, and the result is shown in Fig. 10. The change of pH was also monitored in the presence of various anions (Table 3), excepted  $\text{HCO}_3^-$ , the nearly equivalent initial pH and similar pH variation suggested pH presented the marginal effect in BPA degradation

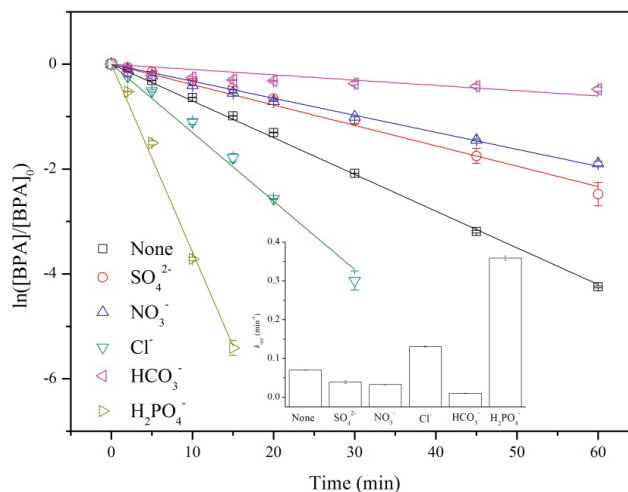


Fig. 10. The effect of anions on BPA removal. Experimental condition:  $[\text{BPA}]_0 = 20 \text{ mg}\cdot\text{L}^{-1}$ ,  $[\text{PMS}]_0 = 0.5 \text{ mM}$ ,  $[\text{Co}_3\text{O}_4\text{-CoMn}_2\text{O}_4]_0 = 0.05 \text{ g}\cdot\text{L}^{-1}$ ,  $[\text{anions}] = 10 \text{ mM}$ ,  $T = 25^\circ\text{C}$ .

Table 3

The variation of solution pH in the BPA degradation with addition of different anions

	None	$\text{SO}_4^{2-}$	$\text{NO}_3^-$	$\text{Cl}^-$	$\text{HCO}_3^-$	$\text{H}_2\text{PO}_4^-$
Initial pH	6.13	6.11	6.14	6.08	7.85	5.12
0 min pH (after PMS addition)	3.62	3.64	3.60	3.62	7.28	3.76
Final pH	3.48	3.52	3.52	3.55	7.17	3.63

when the occurrence of  $\text{SO}_4^{2-}$ ,  $\text{NO}_3^-$ ,  $\text{Cl}^-$  or  $\text{H}_2\text{PO}_4^-$ . From Fig. 10, it can be seen that anions show different influences on BPA removal.  $\text{Cl}^-$  and  $\text{H}_2\text{PO}_4^-$  improved the BPA decomposition, while  $\text{SO}_4^{2-}$ ,  $\text{NO}_3^-$  and  $\text{HCO}_3^-$  inhibited it, and the inhibition extent followed an order of  $\text{HCO}_3^- > \text{NO}_3^- > \text{SO}_4^{2-}$ .

It is well known that  $\text{HCO}_3^-$  is an efficient scavenger to quench  $\text{SO}_4^{\cdot-}$  and  $\cdot\text{OH}$  (Eqs. (19) and (20)) [51], so the decrease of radicals species caused by  $\text{HCO}_3^-$  should be responsible for inhibition of BPA degradation. Besides,  $\text{HCO}_3^-$  can also influence the solution pH, it can be seen that the solution still kept the alkalinescence after PMS addition (Table 3). Thus, it might be another reason for the degradation retarding. And the detrimental effect of  $\text{HCO}_3^-$  was also reported in previous investigations [52–54]. Similarly,  $\text{NO}_3^-$  can also react with  $\text{SO}_4^{\cdot-}$  or  $\cdot\text{OH}$  to produce the species with lower oxidizing ability ( $\text{NO}_3\cdot$ ; 2–2.2 V) (Eqs. (21) and (22)) [55].  $\text{SO}_4^{2-}$  in the heterogeneous activation process will reduce the value of  $E_{(\text{SO}_4^{\cdot-}/\text{SO}_4^{2-})}$ , and a higher  $\text{SO}_4^{2-}$  concentration would result in a lower potential of  $E_{(\text{SO}_4^{\cdot-}/\text{SO}_4^{2-})}$  [56], thereby BPA decay was suppressed when  $\text{SO}_4^{2-}$  in the solution. The similar negative effects caused by  $\text{NO}_3^-$  and  $\text{SO}_4^{2-}$  could also be found in PS activation processes [57,58].

Previous investigations reported that  $\text{Cl}^-$  could be transformed to  $\text{HOCl}$  and  $\text{Cl}_2$  in the presence of PMS (Eqs. (23) and (24)) [59,60]. The formed  $\text{HOCl}$  and  $\text{Cl}_2$  may be the promoter to the BPA removal. And Yao et al. [61] also reported that the decolorization of Orange II would be accelerated in the presence of  $\text{Cl}^-$  in  $\text{MnFe}_2\text{O}_4/\text{PMS}$  and  $\text{MnFe}_2\text{O}_4\text{-rGO}/\text{PMS}$  systems. Besides, Lou et al. [62] disclosed that PMS/ $\text{Cl}^-$  system can remove rhodamine B efficiently, and the higher  $\text{Cl}^-$  concentration and PMS dosage were benefited for organics decomposition. In addition, Zhou et al. [63] compared the effect of  $\text{Cl}^-$  with  $\text{NO}_3^-$  in the PMS activation, and found that 4-chloro-2-nitrophenol degradation would be significantly promoted when the concentration of  $\text{Cl}^-$  was 500 mM, but the same dosage of  $\text{NO}_3^-$  still inhibited the degradation. It might be ascribed to that  $\text{NO}_3^-$  cannot activate PMS to form active species.

Yang et al. [18] investigated PMS activated by various anions and found  $\text{H}_2\text{PO}_4^-/\text{PMS}$  system can remove Acid Orange 7 efficiently, and the performance of  $\text{HPO}_4^{2-}$  was stronger than  $\text{Cl}^-$  in PMS activation. Thus, this maybe the reason for why  $\text{H}_2\text{PO}_4^-$  showed the higher promotion than  $\text{Cl}^-$  in our case. In addition, Lou et al. [64] documented that contaminants can be degraded through phosphate ions activated PMS, and successfully testified that  $\text{SO}_4^{\cdot-}$  and  $\cdot\text{OH}$  may be the major radicals in phosphate ions activated PMS processes.

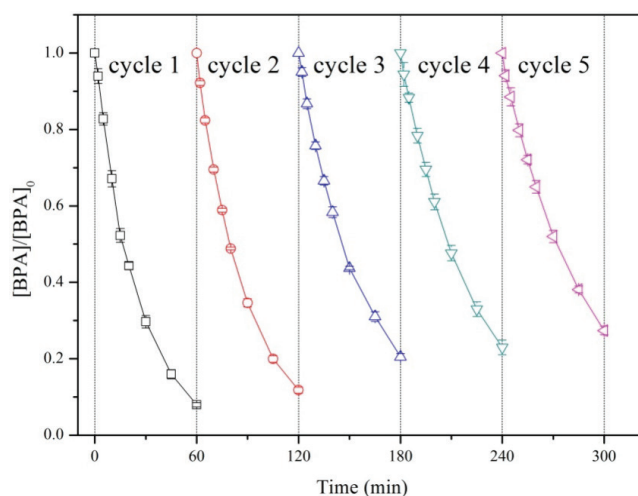
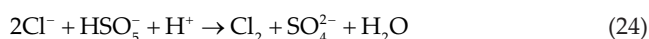
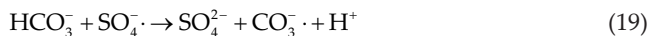


Fig. 11. Catalyst recycling on degradation of BPA. Experimental condition:  $[\text{BPA}]_0 = 20 \text{ mg}\cdot\text{L}^{-1}$ ,  $[\text{PMS}] = 0.5 \text{ mM}$ ,  $[\text{Co}_3\text{O}_4\text{-CoMn}_2\text{O}_4] = 0.05 \text{ g}\cdot\text{L}^{-1}$ ,  $T = 25^\circ\text{C}$ .

### 3.9. Reusability of $\text{Co}_3\text{O}_4\text{-CoMn}_2\text{O}_4$

The catalyst was recycled five runs to evaluate the stability of  $\text{Co}_3\text{O}_4\text{-CoMn}_2\text{O}_4$ , and the results are shown in Fig. 11. After every experiment, the  $\text{Co}_3\text{O}_4\text{-CoMn}_2\text{O}_4$  was collected, washed with distilled water and ethanol several times, and dried at  $70^\circ\text{C}$  to be reused in next run. In each run, BPA removal rate was 92.03%, 88.20%, 79.49%, 77.04% and 72.63% at 60 min, respectively. The catalytic activity of  $\text{Co}_3\text{O}_4\text{-CoMn}_2\text{O}_4$  would decrease with the increase of the number of cycle reusability. But the BPA removal is still satisfied if the reactive time was extended. The leaching of metal ion on the  $\text{Co}_3\text{O}_4\text{-CoMn}_2\text{O}_4$  surface is likely the reason caused the decline of BPA removal. The change of transition metal valence state on the catalyst surface may be the other reason.

## 4. Conclusion

$\text{Co}_3\text{O}_4\text{-CoMn}_2\text{O}_4$  was prepared through an impregnation-calcination method and compared with ordered mesoporous  $\text{Co}_3\text{O}_4$ . There was no obvious difference between  $\text{Co}_3\text{O}_4\text{-CoMn}_2\text{O}_4$  and ordered mesoporous  $\text{Co}_3\text{O}_4$  evidencing by XRD, TEM, HR-TEM and BET, but  $\text{Co}_3\text{O}_4\text{-CoMn}_2\text{O}_4$  had lower toxicity and cost, than ordered mesoporous  $\text{Co}_3\text{O}_4$ . Higher catalyst dosage, PMS concentration and reactive temperature would surely promote the BPA degradation. A wide pH range (5–9) was beneficial for the BPA removal. Different anions presented different results to BPA degradation. It was evidenced that  $\text{SO}_4^{\cdot-}$  was the primary active species and possible mechanism was proposed. After five cycles,  $\text{Co}_3\text{O}_4\text{-CoMn}_2\text{O}_4$  remained relatively stable catalytic activity. In consideration of cost and toxicity,  $\text{Co}_3\text{O}_4\text{-CoMn}_2\text{O}_4/\text{PMS}$  system should have a great potential in environmental cleanup.

## Acknowledgments

The authors would like to acknowledge the financial support from the National Natural Science Foundation of China (51508509, 51678527, 51378446), the China

Postdoctoral Science Foundation (2015M581936) and the Zhejiang Provincial Natural Science Foundation of China (LY18E080036).

## References

- [1] M.F. Sweeney, N. Hasan, A.M. Soto, C. Sonnenschein, Environmental endocrine disruptors: effects on the human male reproductive system, *Rev. Endocr. Metab. Disord.*, 16 (2016) 341–357.
- [2] J. Jurewicz, M. Radwan, W. Sobala, P. Radwan, L. Jakubowski, B. Wielgomas, D. Ligocka, S. Brzenicki, W. Hanke, Exposure to widespread environmental endocrine disrupting chemicals and human sperm sex ratio, *Environ. Pollut.*, 213 (2016) 732–740.
- [3] E.G. Xu, P.W. Ho, Z. Tse, S.L. Ho, K.M.Y. Leung, Revealing ecological risks of priority endocrine disrupting chemicals in four marine protected areas in Hong Kong through an integrative approach, *Environ. Pollut.*, 215 (2016) 103–112.
- [4] Y.Q. Huang, C.K.C. Wong, J.S. Zheng, H. Bouwman, R. Barra, B. Wahlstrom, L. Neretin, M.H. Wong, Bisphenol A (BPA) in China: a review of sources, environmental levels, and potential human health impacts, *Environ. Int.*, 42 (2012) 91–99.
- [5] L.H. You, V.T. Nguyen, A. Pal, H.T. Chen, Y.L. He, M. Reinhard, K.Y.H. Gin, Investigation of pharmaceuticals, personal care products and endocrine disrupting chemicals in tropical urban catchment and the influence of environmental factors, *Sci. Total Environ.*, 536 (2015) 955–963.
- [6] G.D. Wang, P. Ma, Q. Zhang, J. Lewis, M. Lacey, Y. Furukawa, S.E. O'Reilly, S. Meaux, J. McLachlan, S. Zhang, Endocrine disrupting chemicals in New Orleans surface waters and Mississippi Sound sediments, *J. Environ. Monit.*, 14 (2012) 1353–1364.
- [7] J.H. Kang, F. Kondo, Y. Katayama, Human exposure to bisphenol A, *Toxicology*, 226 (2006) 79–89.
- [8] G.P. Anipsitakis, D.D. Dionysiou, Radical generation by the interaction of transition metals with common oxidants, *Environ. Sci. Technol.*, 38 (2004) 3705–3712.
- [9] J. Deng, Y.S. Shao, N.Y. Gao, C.Q. Tan, S.Q. Zhou, X.H. Hu,  $\text{CoFe}_2\text{O}_4$  magnetic nanoparticles as highly active heterogeneous catalyst of oxone for the degradation of diclofenac in water, *J. Hazard. Mater.*, 262 (2013) 836–844.
- [10] P.D. Hu, M.C. Long, Cobalt-catalyzed sulfate radical-based advanced oxidation: a review on heterogeneous catalysts and applications, *Appl. Catal., B*, 181 (2016) 103–117.
- [11] J. Deng, Y.S. Shao, N.Y. Gao, S.J. Xia, C.Q. Tan, S.Q. Zhou, X.H. Hu, Degradation of the antiepileptic drug carbamazepine upon different UV-based advanced oxidation processes in water, *Chem. Eng. J.*, 222 (2013) 150–158.
- [12] C.Q. Tan, D.F. Fu, N.Y. Gao, Q.D. Qin, Y. Xu, H.M. Xiang, Kinetic degradation of chloramphenicol in water by UV/persulfate system, *J. Photochem. Photobiol., A*, 332 (2017) 406–412.
- [13] W.H. Chu, D.M. Li, N.Y. Gao, M.R. Templeton, C.Q. Tan, Y.Q. Gao, The control of emerging haloacetamide DBP precursors with UV/persulfate treatment, *Water Res.*, 72 (2015) 340–348.
- [14] J. Deng, Y.S. Shao, N.Y. Gao, Y. Deng, S.Q. Zhou, X.H. Hu, Thermally activated persulfate (TAP) oxidation of antiepileptic drug carbamazepine in water, *Chem. Eng. J.*, 228 (2013) 765–771.
- [15] W.H. Chu, J.L. Hu, T. Bond, N.Y. Gao, B. Xu, D.Q. Yin, Water temperature significantly impacts the formation of iodinated haloacetamides during persulfate oxidation, *Water Res.*, 98 (2016) 47–55.
- [16] S.N. Su, W.L. Guo, C.L. Yi, Y.Q. Leng, Z.M. Ma, Degradation of amoxicillin in aqueous solution using sulphate radicals under ultrasound irradiation, *Ultrason. Sonochem.*, 19 (2012) 469–474.
- [17] O.S. Furman, A.L. Teel, R.J. Watts, Mechanism of base activation of persulfate, *Environ. Sci. Technol.*, 44 (2010) 6423–6428.
- [18] S.Y. Yang, P. Wang, X. Yang, L. Shan, W.Y. Zhang, X.T. Shao, R. Niu, Degradation efficiencies of azo dye Acid Orange 7 by the interaction of heat, UV and anions with common oxidants: persulfate, peroxymonosulfate and hydrogen peroxide, *J. Hazard. Mater.*, 179 (2010) 552–558.
- [19] Y.X. Wang, Z.M. Ao, H.Q. Sun, X.G. Duan, S.B. Wang, Activation of peroxymonosulfate by carbonaceous oxygen groups: experimental and density functional theory calculations, *Appl. Catal., B*, 198 (2016) 295–302.
- [20] J. Kang, X.G. Duan, L. Zhou, H.Q. Sun, M.O. Tade, S.B. Wang, Carbocatalytic activation of persulfate for removal of antibiotics in water solutions, *Chem. Eng. J.*, 288 (2016) 399–405.
- [21] P.H. Shao, X.G. Duan, J. Xu, J.Y. Tian, W.X. Shi, S.S. Gao, M.J. Xu, F.Y. Cui, S.B. Wang, Heterogeneous activation of peroxymonosulfate by amorphous boron for degradation of bisphenol S, *J. Hazard. Mater.*, 322 (2017) 532–539.
- [22] X.G. Duan, H.Q. Sun, Z.M. Ao, L. Zhou, G.X. Wang, S.B. Wang, Unveiling the active sites of graphene-catalyzed peroxymonosulfate activation, *Carbon*, 107 (2016) 371–378.
- [23] G.P. Anipsitakis, D.D. Dionysiou, Degradation of organic contaminants in water with sulfate radicals generated by the conjunction of peroxymonosulfate with cobalt, *Environ. Sci. Technol.*, 37 (2003) 4790–4797.
- [24] K. Liu, J.H. Lu, Y.F. Ji, Formation of brominated disinfection by-products and bromate in cobalt catalyzed peroxymonosulfate oxidation of phenol, *Water Res.*, 84 (2015) 1–7.
- [25] G.P. Anipsitakis, E. Stathatos, D.D. Dionysiou, Heterogeneous activation of oxone using  $\text{Co}_3\text{O}_4$ , *J. Phys. Chem. B*, 109 (2005) 13052–13055.
- [26] X.Y. Chen, J.W. Chen, X.L. Qiao, D.G. Wang, X.Y. Cai, Performance of nano- $\text{Co}_3\text{O}_4$ /peroxymonosulfate system: kinetics and mechanism study using Acid Orange 7 as a model compound, *Appl. Catal., B*, 80 (2008) 116–121.
- [27] Y.T. Zhang, C. Liu, B.B. Xu, F. Qi, W. Chu, Degradation of benzotriazole by a new novel Fenton-like reaction with mesoporous  $\text{Cu/MnO}_2$ : combination of absorption and catalysis oxidation, *Appl. Catal., B*, 199 (2016) 447–457.
- [28] Y.B. Ding, L.H. Zhu, N. Wang, H.Q. Tang, Sulfate radicals induced degradation of tetrabromobisphenol A with nanoscaled magnetic  $\text{CuFe}_2\text{O}_4$  as heterogeneous catalyst of peroxymonosulfate, *Appl. Catal., B*, 129 (2013) 153–162.
- [29] Y.J. Yao, Y.M. Cai, G.D. Wu, F.Y. Wei, X.Y. Li, H. Chen, S.B. Wang, Sulfate radicals induced from peroxymonosulfate by cobalt manganese oxides ( $\text{Co}_2\text{Mn}_3\text{O}_8$ ) for Fenton-like reaction in water, *J. Hazard. Mater.*, 296 (2015) 128–137.
- [30] J. Deng, S.F. Feng, K.J. Zhang, J. Li, H.Y. Wang, T.Q. Zhang, X.Y. Ma, Heterogeneous activation of peroxymonosulfate using ordered mesoporous  $\text{Co}_3\text{O}_4$  for the degradation of chloramphenicol at neutral pH, *Chem. Eng. J.*, 308 (2017) 505–515.
- [31] T. Grewe, X.H. Deng, C. Weidenthaler, F. Schuth, H. Tuysuz, Design of ordered mesoporous composite materials and their electrocatalytic activities for water oxidation, *Chem. Mater.*, 25 (2013) 4926–4935.
- [32] F. Ji, C.L. Li, X.Y. Wei, J. Yu, Efficient perform porous  $\text{Fe}_2\text{O}_3$  in heterogeneous activation of peroxymonosulfate for decolorization of Rhodamine B, *Chem. Eng. J.*, 231 (2013) 434–440.
- [33] J. Deng, S.F. Feng, X.Y. Ma, C.Q. Tan, H.Y. Wang, S.Q. Zhou, T.Q. Zhang, J. Li, Heterogeneous degradation of Orange II with peroxymonosulfate activated by ordered mesoporous  $\text{MnFe}_2\text{O}_4$ , *Sep. Purif. Technol.*, 167 (2016) 181–189.
- [34] T. Zhang, H.B. Zhu, J.P. Croue, Production of sulfate radical from peroxymonosulfate induced by a magnetically separable  $\text{CuFe}_2\text{O}_4$  spinel in water: efficiency, stability, and mechanism, *Environ. Sci. Technol.*, 47 (2013) 2784–2791.
- [35] Y.M. Ren, L.Q. Lin, J. Ma, J. Yang, J. Feng, Z.J. Fan, Sulfate radicals induced from peroxymonosulfate by magnetic ferrosin  $\text{MFe}_2\text{O}_4$  ( $\text{M} = \text{Co}, \text{Cu}, \text{Mn}, \text{and Zn}$ ) as heterogeneous catalysts in the water, *Appl. Catal., B*, 165 (2015) 572–578.
- [36] Z.H. Ai, Z.T. Gao, L.Z. Zhang, W.W. He, J.J. Yin, Core-shell structure dependent reactivity of  $\text{Fe}@\text{Fe}_2\text{O}_3$  nanowires on aerobic degradation of 4-chlorophenol, *Environ. Sci. Technol.*, 47 (2013) 5344–5352.
- [37] Y. Xu, J. Ai, H. Zhang, The mechanism of degradation of bisphenol A using the magnetically separable  $\text{CuFe}_2\text{O}_4$ /peroxymonosulfate heterogeneous oxidation process, *J. Hazard. Mater.*, 309 (2016) 87–96.

- [38] S.N. Su, W.L. Guo, Y.Q. Leng, C.L. Yi, Z.M. Ma, Heterogeneous activation of Oxone by  $\text{Co}_x\text{Fe}_{3-x}\text{O}_4$  nanocatalysts for degradation of rhodamine B, *J. Hazard. Mater.*, 244–245 (2013) 736–742.
- [39] Y.H. Guan, J. Ma, X.C. Li, J.Y. Fang, L.W. Chen, Influence of pH on the formation of sulfate and hydroxyl in the UV/peroxymonosulfate system, *Environ. Sci. Technol.*, 45 (2011) 9308–9314.
- [40] E. Saputra, S. Muhammad, H.Q. Sun, H.M. Ang, M.O. Tade, S.B. Wang, Manganese oxides at different oxidation states for heterogeneous activation of peroxymonosulfate for phenol degradation in aqueous solutions, *Appl. Catal., B*, 142–143 (2013) 729–735.
- [41] Y.C. Du, W.J. Ma, P.X. Liu, B.H. Zou, J. Ma, Magnetic  $\text{CoFe}_2\text{O}_4$  nanoparticles supported on titanate nanotubes ( $\text{CoFe}_2\text{O}_4/\text{TNTs}$ ) as a novel heterogeneous catalyst for peroxymonosulfate activation and degradation of organic pollutants, *J. Hazard. Mater.*, 308 (2016) 58–66.
- [42] F. Qi, W. Chu, B.B. Xu, Catalytic degradation caffeine in aqueous solutions by cobalt-MCM41 activation of peroxymonosulfate, *Appl. Catal., B*, 134–135 (2013) 324–332.
- [43] L.J. Xu, W. Chu, L. Gan, Environmental application of graphene-based  $\text{CoFe}_2\text{O}_4$  as an activator of peroxymonosulfate for the degradation of a plasticizer, *Chem. Eng. J.*, 263 (2015) 435–443.
- [44] J. Zhang, M.Y. Chen, L. Zhu, Activation of peroxymonosulfate by iron-based catalysts for orange G degradation: role of hydroxylamine, *RSC Adv.*, 6 (2016) 47562–47569.
- [45] S.K. Rani, D. Easwaramoorthy, I.M. Bilal, M. Palanichamy, Studies on Mn(II)-catalyzed oxidation of  $\alpha$ -amino acids by peroxomonosulphate in alkaline medium-deamination and decarboxylation: a kinetic approach, *Appl. Catal., A*, 369 (2009) 1–7.
- [46] J.K. Du, J.G. Bao, Y. Liu, H.B. Ling, H. Zheng, S.H. Kim, D.D. Dionysiou, Efficient activation of peroxymonosulfate by magnetic Mn-MGO for degradation of bisphenol A, *J. Hazard. Mater.*, 320 (2016) 150–159.
- [47] Y. Zhao, Y.S. Zhao, R. Zhou, Y. Mao, W. Tang, H.J. Ren, Insights into the degradation of 2,4-dichlorophenol in aqueous solution by  $\alpha$ - $\text{MnO}_2$  nanowire activated persulfate: catalytic performance and kinetic modeling, *RSC Adv.*, 6 (2016) 35441–35448.
- [48] H. Hassan, B.H. Hammed, Fe-clay as effective heterogeneous Fenton catalyst for the decolorization of Reactive Blue 4, *Chem. Eng. J.*, 171 (2011) 912–918.
- [49] W. Li, P.X. Wu, Y.J. Zhu, Z.J. Huang, Y.H. Lu, Y.W. Li, Z. Dang, N.W. Zhu, Catalytic degradation of bisphenol A by CoMnAl mixed metal oxides catalyzed peroxymonosulfate: performance and mechanism, *Chem. Eng. J.*, 279 (2015) 93–102.
- [50] P.R. Shukla, S.B. Wang, H.Q. Sun, H.M. Ang, M. Tade, Activated carbon supported cobalt catalysts for advanced oxidation of organic contaminants in aqueous solution, *Appl. Catal., B*, 100 (2010) 529–534.
- [51] A. Ghauch, A.M. Tuqan, Oxidation of bisoprolol in heated persulfate/ $\text{H}_2\text{O}$  systems: kinetics and products, *Chem. Eng. J.*, 183 (2012) 162–171.
- [52] Y.J. Xiao, L.F. Zhang, W. Zhang, K.Y. Lim, R.D. Webster, T.T. Lim, Comparative evaluation of iodoacids removal by UV/persulfate and UV/ $\text{H}_2\text{O}_2$  processes, *Water Res.*, 102 (2016) 629–639.
- [53] C.Q. Tan, N.Y. Gao, D.F. Fu, J. Deng, L. Deng, Efficient degradation of paracetamol with nanoscaled magnetic  $\text{CoFe}_2\text{O}_4$  and  $\text{MnFe}_2\text{O}_4$  as a heterogeneous catalyst of peroxymonosulfate, *Sep. Purif. Technol.*, 175 (2017) 47–57.
- [54] X.Y. Wei, N.Y. Gao, C.J. Li, Y. Deng, S.Q. Zhou, L. Li, Zero-valent iron (ZVI) activation of persulfate (PS) for oxidation of bentazon in water, *Chem. Eng. J.*, 285 (2016) 660–670.
- [55] T. Zhou, X.L. Zou, J. Mao, X.H. Wu, Decomposition of sulfadiazine in sonochemical  $\text{Fe}^0$ -catalyzed persulfate system: parameters optimizing and interferences of wastewater matrix, *Appl. Catal., B*, 185 (2016) 31–41.
- [56] X.L. Wu, X.G. Gu, S.G. Lu, Z.F. Qiu, Q. Sui, X.K. Zang, Z.W. Miao, M.H. Xu, Strong enhancement of trichloroethylene degradation in ferrous ion activated persulfate system by promoting ferric and ferrous ion cycles with hydroxylamine, *Sep. Purif. Technol.*, 147 (2015) 186–193.
- [57] Y.F. Rao, L. Qu, H.S. Yang, W. Chu, Degradation of carbamazepine by Fe(II)-activated persulfate process, *J. Hazard. Mater.*, 268 (2014) 23–32.
- [58] Y.Q. Gao, N.Y. Gao, Y. Deng, D.Q. Yin, Y.S. Zhang, W.L. Rong, S.D. Zhou, Heat-activated persulfate oxidation of sulfamethoxazole in water, *Desal. Wat. Treat.*, 56 (2015) 2225–2233.
- [59] R.X. Yuan, S.N. Ramjaun, Z.H. Wang, J.S. Liu, Effects of chloride ion on degradation of Acid Orange 7 by sulfate radical-based advanced oxidation process: implications for formation of chlorinated aromatic compounds, *J. Hazard. Mater.*, 196 (2011) 173–179.
- [60] F. Gong, L. Wang, D.W. Li, F.Y. Zhou, Y.Y. Yao, W.Y. Lu, S.Q. Huang, W.X. Chen, An effective heterogeneous iron-based catalyst to activate peroxymonosulfate for organic contaminants removal, *Chem. Eng. J.*, 267 (2015) 102–110.
- [61] Y.J. Yao, Y.M. Cai, F. Lu, F.Y. Wei, X.Y. Wang, S.B. Wang, Magnetic recoverable  $\text{MnFe}_2\text{O}_4$  and  $\text{MnFe}_2\text{O}_4$ -graphene hybrid as heterogeneous catalysts of peroxymonosulfate activation for efficient degradation of aqueous organic pollutants, *J. Hazard. Mater.*, 270 (2014) 61–70.
- [62] X.Y. Lou, Y.G. Guo, D.X. Xiao, Z.H. Wang, S.Y. Lu, J.S. Liu, Rapid dye degradation with reactive oxidants generated by chloride-induced peroxymonosulfate activation, *Environ. Sci. Pollut. Res.*, 20 (2013) 6317–6323.
- [63] J. Zhou, J.H. Xiao, D.X. Xiao, Y.G. Guo, C.L. Fang, X.Y. Lou, Z.H. Wang, J.S. Liu, Transformations of chloro and nitro groups during the peroxymonosulfate-based oxidation of 4-chloro-2-nitrophenol, *Chemosphere*, 134 (2015) 446–451.
- [64] X.Y. Lou, L.X. Wu, Y.G. Guo, C.C. Chen, Z.H. Wang, D.X. Xiao, C.L. Fang, G.S. Liu, J.C. Zhao, S.Y. Lu, Peroxymonosulfate activation by phosphate anion for organics degradation in water, *Chemosphere*, 117 (2014) 582–585.